

Chapter 2

Equipment and Material Flow Control

Abstract Process control ensures that stamped part quality is maintained in the presence of operational variations and disturbances. Control objectives are achieved by adjusting the flow of metal into the die cavity in response to these variations and disturbances. This chapter provides an overview of the process and equipment used for sheet-metal stamping, and describes the methods through which material flow control can be effected during the stamping process. Simplified kinematic and dynamic models for press motion are derived, followed by a description of hydraulic actuation to implement variable binder force for material flow control.

2.1 Types of Stamping Presses

The sheet metal stamping process, described in [Sect. 1.3](#), will now be explored in greater detail. We begin with an overview of the two main types of stamping presses that are commonly used in the manufacture of deep-drawn parts, namely, *mechanical presses* and (*electro-*) *hydraulic presses*.

Metal-forming presses are used for a number of operations including deep-drawing, blanking and trimming. A typical *press-line* in a production facility has several presses in a line, each of which performs one or more operations on a part, with automation sequentially moving the part along the line. Our study will be confined to presses used for drawing.

As seen in [Fig. 1.4](#), for drawing, the punch has to be driven by a mechanism to force the blank into the die. Mechanical presses use a linked-drive powered by an electric motor to drive the punch. A clutch mechanism is used to engage or disengage the drive, and a braking system is included to stop the drive. Hydraulic presses use hydraulic cylinders to drive the punch. Servo-valves or proportional valves are utilized to control the flow of pressurized hydraulic fluid into the cylinders during the punch stroke.

The two main characteristics of a press that affect the forming process are the *press tonnage*, which is the maximum force applied by the press on the blank (typically at the bottom of the forming stroke) and the *press curve*, which is the variation of the speed of the punch during the forming stroke. Most modern presses have sensors, or load-cells, called *tonnage monitors*, which measure the press tonnage at the four corners of the press. In a mechanical press, the press curve is determined by the kinematics of the drive mechanism, while for a hydraulic press, the punch speed is constant until the punch slows down close to the bottom of the stroke. However, modern *electro-hydraulic servo-presses* allow the operators to program desired press curves to enable better forming control.

The rate at which a press runs, specified in *strokes per minute*, determines the production rate, while the *shut-height* of the press, which is the vertical displacement of the punch as it impacts the blank, determines the size of the die that can be accommodated in a press for a given draw depth.

Presses, both mechanical and electro-hydraulic can be either *single-acting* or *double-acting*. In a single-acting press, the drive mechanism only moves the press ram, while in a double-acting press, the drive mechanism moves an outer blank-holding ring which clamps the blank before it drives the press ram to form the metal. Variable binder-force control is more effective in single-acting presses, and thus, our discussion in this book will be limited to these presses.

2.2 Mechanical Presses

The basic functional components in a mechanical press are shown in Fig. 2.1. The drive mechanism consists of an electric motor connected to a crank mechanism to move the punch along a guide on the sides of the press-frame (Adam et al. 1998). We now develop a simplified model of the kinematics of a mechanical press.

Referring to Fig. 2.2, we see that

$$y(t) = R \cos(\theta(t)) + \sqrt{l^2 - R^2 \sin^2 \theta(t)} \quad (2.1)$$

and differentiating (2.1) with respect to time yields

$$\dot{y}(t) = -R \sin(\theta(t))\omega - \frac{R^2 \sin(2\theta(t))\omega}{2\sqrt{l^2 - R^2 \sin^2 \theta(t)}} \quad (2.2)$$

where t denotes time and $\omega = \dot{\theta}(t)$ denotes the constant angular speed of the press-drive, with a super-scripted dot indicating the time-derivative of a time-dependent function.

Figure 2.3 shows the simulated press-curve of the press-drive modeled above, with $\omega = 2.0944$ rad/s, corresponding to a press running at 20 strokes/min, and $R = 0.5$ m, $l = 2.5$ m. Note that the speed of punch decreases rapidly as the punch reaches the bottom of the stroke, ensuring that the final stages of forming are achieved at a lower strain rate.

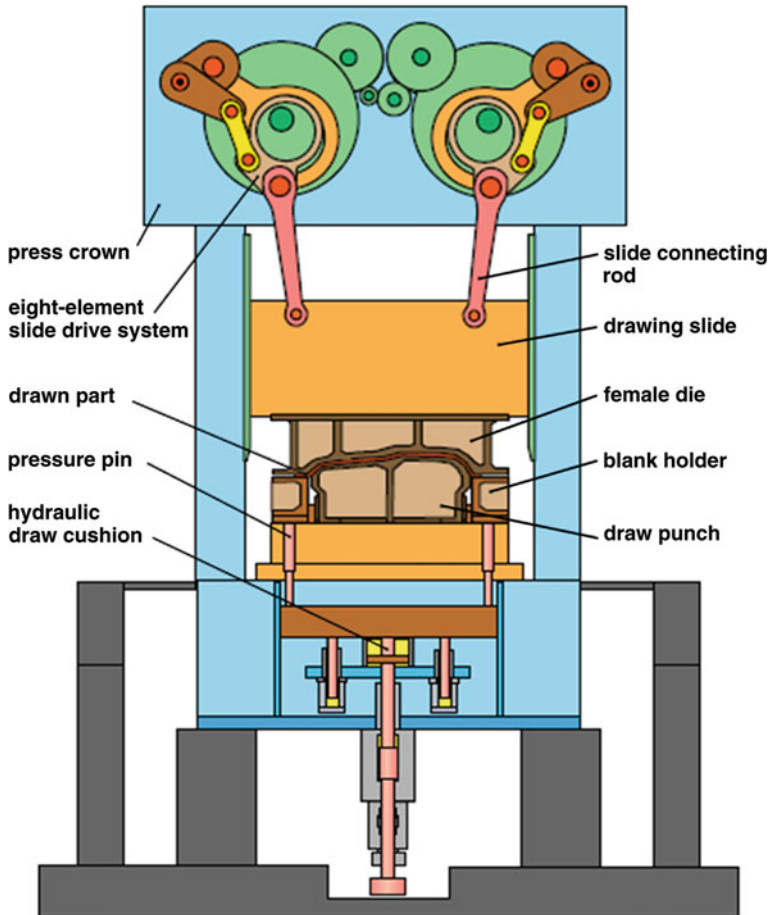


Fig. 2.1 Components of a mechanical press

2.3 Hydraulic Presses

Hydraulic (or electro-hydraulic) presses are also used for deep-drawing sheet metal. In contrast to mechanical presses, the driving force of the press is generated by pressurized hydraulic fluid. The press ram is driven by hydraulic cylinders attached to the press ram as shown in Fig. 2.4.

A simplified mathematical model to derive the press ram-speed, $\dot{y}(t)$, as a function of the supply pressure, P_s , the bulk-modulus of the hydraulic fluid, β , the density of the hydraulic fluid, ρ , the cross-sectional areas of the hydraulic cylinder in contact with the fluid on the rod-side and the blind-side, A_1 and A_2 respectively, the servo-valve effective flow-area, K_v , and the total length of the cylinder, l , is shown below.

Fig. 2.2 Simplified schematic of an eccentric drive for a mechanical press

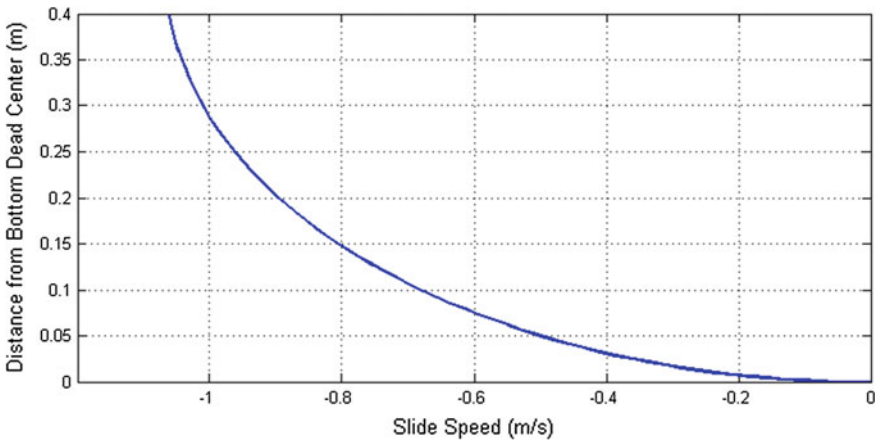
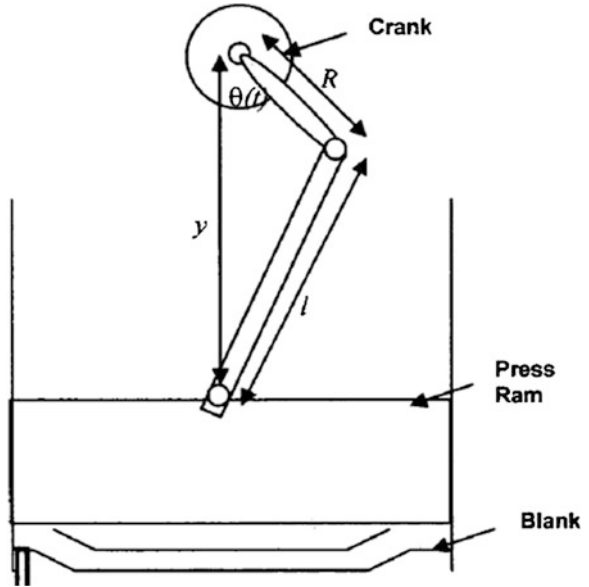


Fig. 2.3 Simulated mechanical press curve

Referring to the simplified schematic in Fig. 2.5, the pressurized hydraulic fluid enters one side of the double-acting hydraulic cylinders via servo-valves. The return flow from the other side of the cylinders is handled by the same servo-valves.

First, the change in pressure in a hydraulic fluid, ΔP , is related to the bulk-modulus, volumetric change, ΔV , and the instantaneous volume of the hydraulic fluid, $V(t)$, by (Merrit 1991)

Fig. 2.4 Components of a hydraulic press

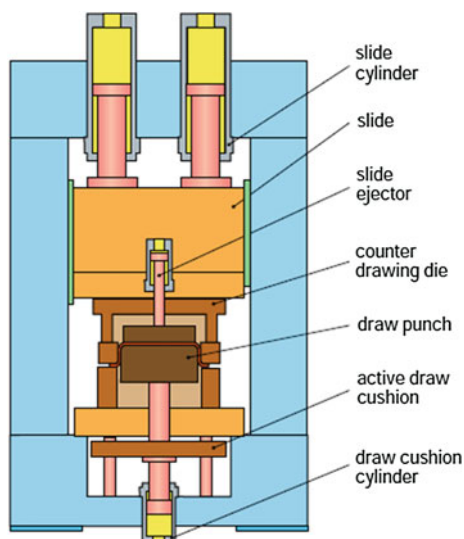
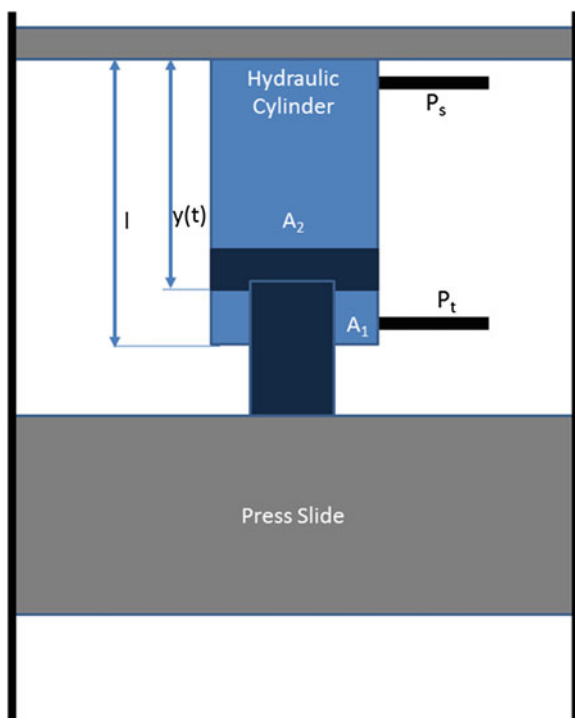


Fig. 2.5 Simplified schematic of hydraulic press drive



$$\Delta P = -\beta \frac{\Delta V}{V(t)} \quad (2.3)$$

or,

$$\dot{P}(t) = -\beta \frac{\dot{V}(t)}{V(t)}. \quad (2.4)$$

Denoting the pressure of the hydraulic cylinder on the rod-side as P_1 and that on the blind-side as P_2 , assuming laminar flow and using Bernoulli's equation, the rate of hydraulic fluid flow into the blind-side of the cylinder, $Q_2(t)$, is given by

$$Q_2(t) = K_v \sqrt{\frac{2(P_s - P_2)}{\rho}} \quad (2.5)$$

and thus, the net rate of change of volume of the hydraulic fluid in the blind-side, $\dot{V}_2(t)$, taking into account the vertical motion of the piston, is

$$\dot{V}_2(t) = Q_2(t) - A_2 \dot{y}(t) \quad (2.6)$$

or,

$$\dot{V}_2(t) = K_v \sqrt{\frac{2(P_s - P_2)}{\rho}} - A_2 \dot{y}(t). \quad (2.7)$$

Similarly, using analogous notation for the rod-side, it can be shown that

$$\dot{V}_1(t) = A_1 \dot{y}(t) - K_v \sqrt{\frac{2(P_1)}{\rho}} \quad (2.8)$$

assuming that the tank pressure is 0.

Next, using (2.4), (2.7) and (2.8), it follows that

$$\dot{P}_1(t) = \beta \frac{A_1 \dot{y}(t) - K_v \sqrt{\frac{2(P_1)}{\rho}}}{A_1(l - y(t))} \quad (2.9)$$

and

$$\dot{P}_2(t) = \beta \frac{K_v \sqrt{\frac{2(P_s - P_2)}{\rho}} - A_2 \dot{y}(t)}{A_2 y(t)}. \quad (2.10)$$

Finally, letting m denote the mass of the slide and punch and invoking Newton's Second Law of Motion, it follows that

$$m \ddot{y}(t) = P_2 A_2 - P_1 A_1. \quad (2.11)$$

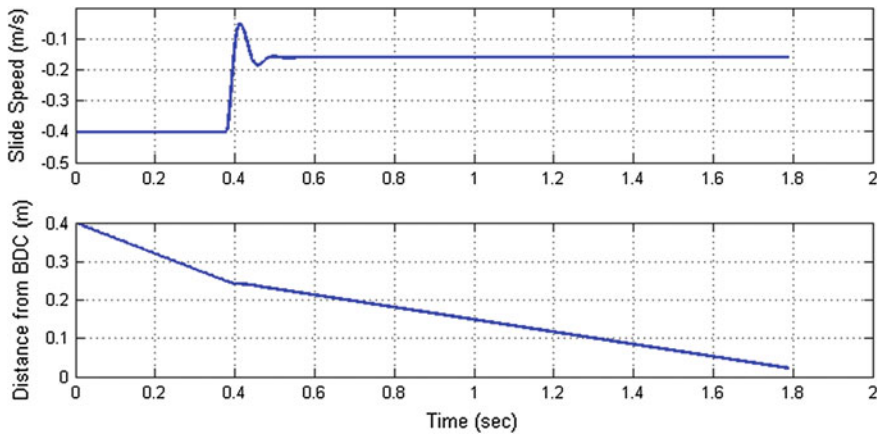


Fig. 2.6 Simulated slide speed profile for a hydraulic press

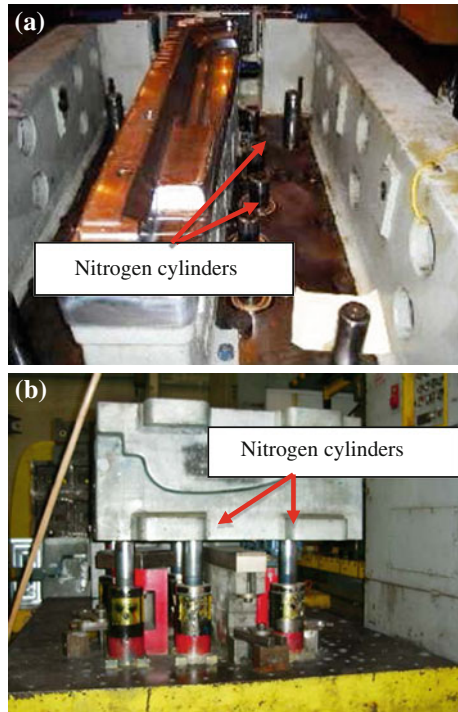
The press ram-speed, $\dot{y}(t)$ can thus be calculated by numerically integrating Eqs. (2.9), (2.10) and (2.11).

Figure 2.6 shows a simulated slide speed profile for a hydraulic press. The press parameters are as follows: $m = 50$ tons, $P_s = 35$ MPa, $A_1 = 0.15$ m², $A_2 = 0.5$ m², $\beta = 1.25$ GPa, $l = 2.5$ m and $\rho = 850$ kg/m³. The servo-valve is rated at 1,500 l/min at a pressure differential of 0.5 MPa. In contrast to a mechanical press, the speed of the slide can be controlled by regulating the flow of hydraulic fluid into the cylinder using the servo-valve. For a given setting of the spool of the servo-valve, the speed of the cylinder reaches a constant speed. In the upper plot, it can be seen that the slide is lowered at a speed of 0.4 m/s until the ram comes close to contact with the blank and then it is slowed down to a speed of 0.18 m/s for the forming cycle. The corresponding slide displacement is shown in the lower plot. The models derived above to characterize the slide speeds for both mechanical and hydraulic presses are useful in the design of hydraulically actuated variable binder force systems. The binder force is generated by compression of the hydraulic fluid as the binder moves down, and the speed of the binder is the same as the slide speed once the ram comes in contact with the die.

2.4 Variable Binder Force Control

As described in Sect. 1.3, binder force plays an important role in how the material flows during the forming process, and is thus crucial to part quality. Two methods are conventionally used to control material flow; the first utilizes drawbeads which are designed using FEA, while the second uses fixed binder forces applied either using a *draw cushion* or nitrogen cylinders (*nitros*). With both these methods, the material flow cannot be actively changed during the forming process.

Fig. 2.7 **a** Production-out die with nitrogen cylinders installed, **b** try-out die with nitrogen cylinders installed



A draw cushion generates binder force using compressed air or hydraulic fluid located in the bed of the press underneath the die (see Figs. 2.1 and 2.4). The force is transmitted by a number of cushion pins to the binder. As the pressure in the fluid is constant across all pins, the binder force cannot be varied spatially. Furthermore, the pressure in the fluid builds up during the stroke and is typically not controlled. Newer hydraulic press cushions are sometimes segmented into quadrants and allow pressure variation in preset steps, allowing a limited amount of binder force control in both space and time, but these adjustments are typically coarse.

Nitrogen cylinders are passive cylinders with pressurized nitrogen, which are mounted under the binder. Figure 2.7 shows production and try-out dies with nitrogen cylinders installed. The pressure in each cylinder can be adjusted locally to vary binder force, but the force in these cylinders always increases during the stroke, due to compression of the gas. Thus, the total binder force at the end of the stroke, where splits typically occur, is always higher than at the start of the stroke, resulting in limited ability to affect material flow during the stamping cycle.

Extensive research has been conducted on the use of variable binder force for part quality improvement (Hashida and Wagoner 1993; Siegert et al. 1997, 2000; Krishnan and Jian 2003; Hsu et al. 2000, 2002; Lim et al. 2008, 2010, 2012). The most effective method is to vary the binder force locally at a number of points

around the die (typically 12–20) (Lim et al. 2010, 2012) as lightweight materials formed in complex shapes have a tendency to have both splits and wrinkles in different areas.

An effective way of generating binder force that can be varied both spatially and temporally during the stroke is to use a set of hydraulic cylinders. The pressure within each individual cylinder is controlled during the press stroke using high-bandwidth servo-valves. For example, using such a system, the binder force in one location can be maintained at a relatively high level for most of the stroke and then relaxed in the last 1 cm of stroke to prevent a split. At another location, the binder force can be increased in the last 1.5 cm of stroke to reduce spring-back or to create the desired stretch. In Chap. 4, the design of hydraulic actuation systems for variable binder force control will be treated in detail.

It is noted that for local variation of binder force to be effective, the binder has to flex. Several studies have been conducted on the use of flexible binders for improving part quality (Siegert et al. 1997, 2000; Krishnan and Jian 2003). Increased flexibility is achieved through the use of segmented binders. However, more recent studies have shown that standard “rigid” binders show sufficient flexibility to ensure local material flow control with locally varying binder force, in both die try-out and production (Lim et al. 2010, 2012).

Alternative methods of actively controlling material flow during the stamping process include the use of active drawbeads (Li and Weinmann 1999; Bohn et al. 2001) ultrasonic vibrations (Takashi et al. 1998) and electromagnetic impulses (Daehn et al. 1999; Shang and Daehn 2011). With active drawbeads, the bead is segmented and the height of each segment can be adjusted during the stamping cycle to control material flow. Ultrasonic vibrations can also be locally targeted to vary the friction between the blank and the die surface during the forming process, thus allowing local material flow control. Finally, electromagnetic impulses directly affect the strain energy in the material. While all these methods have shown the ability to improve part quality in laboratory studies, they all involve complex actuation mechanisms and their implementation on the shop is currently prohibitively expensive.

2.5 Overview of Machine and Process Control

To close this chapter, the overall control architecture for stamping process control is reviewed. In Sect. 2.4, actuation methods to effect material flow control were described. Each of these methods requires a closed-loop to ensure that the actuator changes the control variable, for example, local binder-force or active draw-bead height, as desired. Once this can be done, an outer process-control loop is used to generate reference commands for the control variable to achieve the desired process-control objectives. The block-diagram in Fig. 2.8 shows the control architecture using hydraulic actuators for variable binder force.

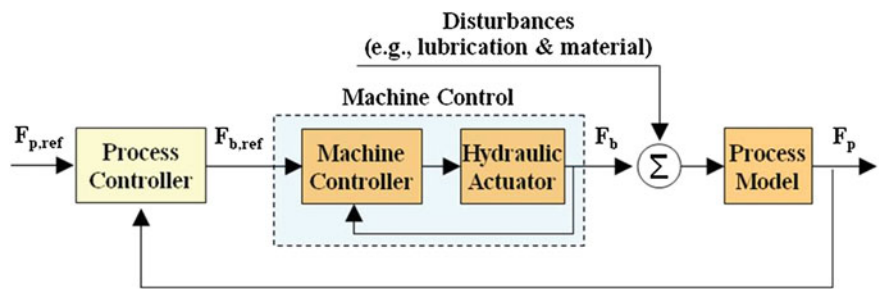


Fig. 2.8 Control architecture for stamping process control

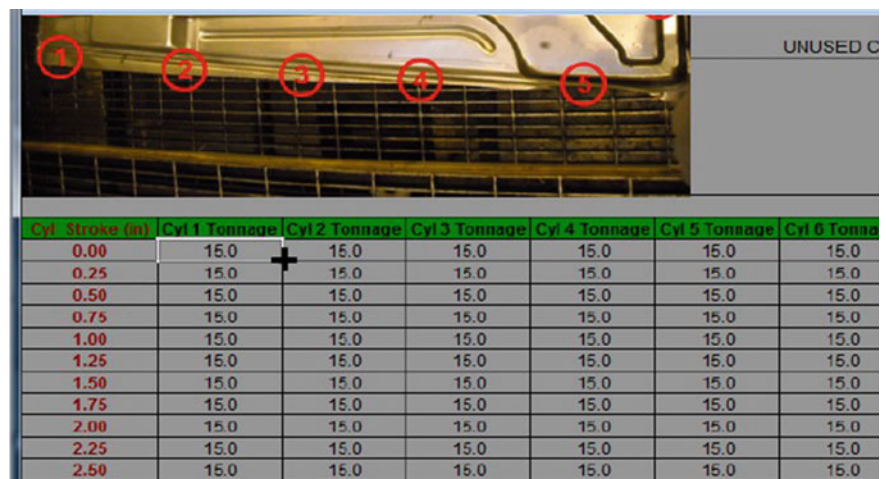


Fig. 2.9 Binder tonnage input user interface

The inner actuation control is achieved using a *machine controller*. All further discussion will be limited to variable binder force systems utilizing hydraulic actuators. Formability can be improved by the use of machine control alone (Lim et al. 2010); a skilled operator manually inputs binder force reference commands ($F_{b,ref}$) for each actuator to correct splits, wrinkles or spring-back. Figure 2.9 shows an input screen for machine control of a commercial 12-cylinder variable binder force system. The binder force applied by each actuator is commanded in 6.35 mm (0.25 inch) increments of punch travel during the forming cycle. The machine controller ensures that these binder force commands are tracked by the actuator and delivered to the binder. The best binder force profiles to make a part of desired quality under nominal conditions are established during try-out. Initial estimates for variable binder force profiles may be generated using FEA prior to try-out (Ahmetoglu et al. 1995; Sheng et al. 2004).

These force profiles create a baseline under nominal conditions. However, operational variations such as changes in lubrication or material properties can result in part defects, if the binder force profiles are maintained at their nominal settings. When such defects occur, the die try-out specialists may be able to adjust the binder force profiles to compensate for the operational variables but such changes are typically made using trial-and-error and may result in unacceptable downtime during a production run. A more robust approach is to use a process control to continually monitor a process variable that reflects part quality and automatically correct the binder force reference commands fed to the machine controller. These corrections modify the nominal binder force commands to ensure that part quality is maintained in the face of operational variations.

The hydraulic dynamics of the actuators induce nonlinearities that need to be addressed in the machine controller. [Chapter 4](#) describes the use of feedback linearization to handle these nonlinearities. The fact that multiple actuators are used with multiple process variable sensors leads to the need to design a multiple-input multiple-output (MIMO) process controller. Furthermore, the number of sensors is usually much lower than the number of actuators, leading to a non-square MIMO structure. The process dynamics are also nonlinear; however, experimental tests indicate that linearized models are sufficient to correct typical part defects that occur in production runs (Lim et al. [2010](#), [2012](#)). [Chapters 6](#), [7](#) and [8](#) describe several methods for process control design, starting with a simple PID approach and moving to direct and indirect adaptive control to handle the large uncertainty in parameters.

References

- Adam, K. et al. (1998) Schuler metal forming handbook. Springer-Verlag, Berlin.
- Ahmetoglu, M., Broek, T. R., Kinzel, G., Altan, T. (1995) Control of blank holder force to eliminate wrinkling and fracture in deep-drawing rectangular parts. *CIRP Annals* 44(1): 247–250
- Bohn, M., Xu, S., Weinmann, K., Chen, C., Chandra, A. (2001) Improving formability in sheet metal stamping with active drawbead technology. *J. of Engineering Materials and Technology* 123: 504–510.
- Daehn, G. S., Vohnout, V. J., DuBois, L. (1999). Improved formability with electromagnetic forming: fundamentals and a practical example. *Minerals, Metals and Materials Society/ AIME, Sheet Metal Forming Technology (USA)*: 105–115.
- Hashida, Y.; Wagoner, R. H. (1993) Experimental analysis of blank holding force control in sheet forming, SAE Paper 930285, Sheet Metal Stamping Symposium, SAE SP-994: 93–100, Warrendale, PA.
- Hsu, C. W., Ulsoy, A. G., Demeri, M. Y. (2000) An approach for modeling sheet metal forming for process controller design. *ASME J. of Manufacturing Science and Engineering* 122(4): 717–724
- Hsu, C. W., Ulsoy, A. G., Demeri, M. Y. (2002) Development of process control in sheet metal forming. *J. of Materials Processing Technology* 127(3): 361–368

- Krishnan, N., Jian, C. (2003). Estimation of optimal blank holder force trajectories in segmented binders using an ARMA model. *Journal of manufacturing science and engineering*, 125(4): 763–770
- Li, R.i, Weinmann, K. J. (1999) Non-symmetric panel forming of AA 6111-T4 using active drawbeads, *Proc. of TMS symposium, San-Diego*, p.39–52
- Lim, Y., Venugopal, R., Ulsoy, A. G. (2008) Advances in the Control of Stamping Processes. *Proc. IFAC World Congress*, 17(1): 1875–1883
- Lim, Y., Venugopal, R., Ulsoy, A. G. (2010) Multi-input multi-output (MIMO) modeling and control for stamping. *ASME J. Dynamic Systems, Measurement and Control* 132(4): 041004 (12 pages)
- Lim, Y., Venugopal, R., Ulsoy, A. G. (2012) Auto-tuning and adaptive stamping process control. *Control Engineering Practice* 20(2): 156–164
- Merritt, H. E. (1991) *Hydraulic control systems*. Wiley, New Jersey
- Shang, J., and Daehn, G. (2011). Electromagnetically assisted sheet metal stamping. *Journal of Materials Processing Technology*, 211(5): 868–874
- Sheng, Z. Q., Jirathearanat, S., Altan, T. (2004) Adaptive FEM simulation for prediction of variable blank holder force in conical cup drawing. *Int. J. of Machine Tools and Manufacture* 44(5): 487–494
- Siegert, K., Altan, T., Nakagawa, T. (1997). Development and manufacture of dies for car body production. *CIRP Annals-Manufacturing Technology*, 46(2): 535–543.
- Siegert, K., Häussermann, M., Haller, D., Wagner, S., Ziegler, M. (2000). Tendencies in presses and dies for sheet metal forming processes. *Journal of Materials Processing Technology*, 98(2): 259–264
- Takashi, J., Yukio, K., Nobuyoshi, I., Osamu, M., Eiji M., Katsuhiko, I., Hajime, H. (1998) An application of ultrasonic vibration to the deep drawing process, *Journal of Materials Processing Technology* 80–81: 406–412

Process Control for Sheet-Metal Stamping
Process Modeling, Controller Design and Shop-Floor
Implementation

Lim, Y.; Venugopal, R.; Ulsoy, A.G.

2014, XI, 140 p. 79 illus., 67 illus. in color., Hardcover

ISBN: 978-1-4471-6283-4